CONFORMATIONAL INFLUENCE ON DEPROTONATION OF BIS(METHOXYCARBIMIDO)AMINE LIGAND

Kateřina BRUDÍKOVÁ[a], Martin BREZA[b,*] and Pavel MÁJEK[c]

[a] *Department of Physical and Applied Chemistry, Brno University of Technology, CZ-612 00 Brno, Czech Republic; e-mail: k.brudikova@email.cz*

[b] *Department of Physical Chemistry, Slovak Technical University, SK-81237 Bratislava, Slovakia; e-mail: breza@cvt.stuba.sk*

[c] *Department of Analytical Chemistry, Slovak Technical University, SK-81237 Bratislava, Slovakia; e-mail:pavel.majek@stuba.sk*

Received August 12, 2004
Accepted October 20, 2004

Dedicated to Professor Vojtech Kellö on the occasion of his 85th birthday.

Using MP2 treatment, the optimal geometries and corresponding electronic structures of $[HN{=}C(OCH_3){-}N{-}C(OCH_3){=}NH]^-$ (mici$^-$), $HN{=}C(OCH_3){-}NH{-}C(OCH_3){=}NH$ (Hmici), $[Cu(mici)]_2$ and $[Cu(Hmici)_2]^{2+}$ were investigated. In agreement with experimental data, the preferred conformation of our systems depends on the ligand: mici$^-$ prefers the methoxy groups oriented to the central N atom whereas Hmici prefers the opposite orientations. The shielding by the methoxy groups is the main reason for the preferred site of deprotonation. The deprotonation of the $[Cu(Hmici)_2]^{2+}$ complex is more probable than that of the free Hmici ligand. Due to preferred conformation of this complex, the deprotonation proceeds by cleavage of the central N–H bond.

Keywords: MP2 geometry optimization; Copper complexes; Bis(methoxycarbimido)amine; Topological analysis of electron density; Ab initio calculations; N-ligands; Imidates.

Transition metal complexes with dicyanamide bridges, $[N(CN)_2]^-$, are promising technological materials due to their interesting magnetic properties[1]. Depending on reaction conditions, the hydrolysis of dicyanamide salts may result in various polymerization products, cyanourea, biuret or, finally, in carbon dioxide and ammonia[2]. $[N(CN)_2]^-$ ions exhibit an enhanced reactivity in the coordination sphere of some metals. In methanolic solutions, the formation of neutral bis(methoxycarbimido)amine molecule, $HN{=}C(OCH_3){-}NH{-}C(OCH_3){=}NH$, or its anion, $[HN{-}C(OCH_3){-}N{-}C(OCH_3){-}NH]^-$ can be observed[1,3–7] (Figs 1 and 2). Both these compounds have been described elsewhere[8]. The nucleophilic addition of methanol to the cyano carbon of co-

ordinated dicyanamide leads to the formation of a six-membered metallacycle[3,4], as indicated by the square-planar structure of $[Cu(mici)_2]$, $mici^-$ = $[HN–C(OCH_3)–N–C(OCH_3)–NH]^-$ (Fig. 3b). Replacing the central atom by the reaction of $[Cu(mici)_2]$ in dimethyl sulfoxide with CoS led to the formation of $[Co(mici)_3]$ (lit.[5]) whereas FeS caused the formation of $[Fe(Hmici)_2(H_2O)(SO_4)]\cdot 2H_2O$, Hmici = $HN=C(OCH_3)–NH–C(OCH_3)=NH$ (lit.[6]), where the metallacycle is formed by the neutral bis(methoxycarbimido)amine ligand. The same neutral ligand is known in the structure of the square-planar $[Cu(Hmici)_2]^{2+}$ complex cation (Fig. 4a) in $[Cu\{bis(methoxycarbimido)amine\}_2(biuret)_2]Br_2\cdot 2biuret\cdot 2MeOH\cdot 0.8MeCN$ (lit.[7]) (obtained from

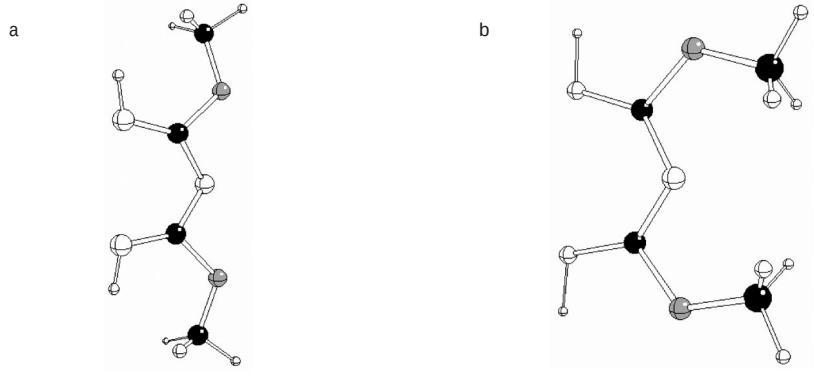

FIG. 1
Structure of $mici^-$: a model A1; b model A2 (for atom notation, see Chart 1)

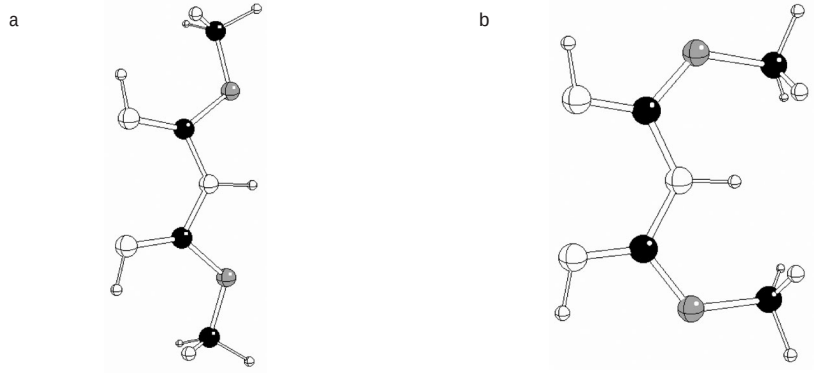

FIG. 2
Structure of Hmici: a model B1; b model B2 (for atom notation, see Chart 1)

its soluble Zn(II) salt in methanol–acetonitrile solution). It is interesting that the methoxy groups in the planar anionic mici$^-$ (in the complexes with Cu(II) (lit.[3,4]) and Co(III) (lit.[5]) and neutral Hmici (in the complexes with Cu(II) (lit.[7]) and Fe(II) (lit.[6])) ligands are in opposite positions (cf. Figs 3b and 4a).

Related complexes of the biuretate dianion ligand, [HN–CO–NH–CO–NH]$^{2-}$, such as $[Cu(biuret)_2]^{2-}$ (lit.[9]), $[Co(biuret)_3]^{3-}$ (lit.[10]) and $[Ni(biuret)_2]^{2-}$ (lit.[11]), are known but we have not found any structural data on transition metal complexes with its anionic analogue in the Cambridge Structure Database[12].

It is evident that the relative stability of transition metal complexes with neutral Hmici and anionic mici$^-$ ligands depends on a delicate balance between intrinsic properties of the complex (such as electronic structure) and influence of the solvent (such as pH). Here the question arises whether the

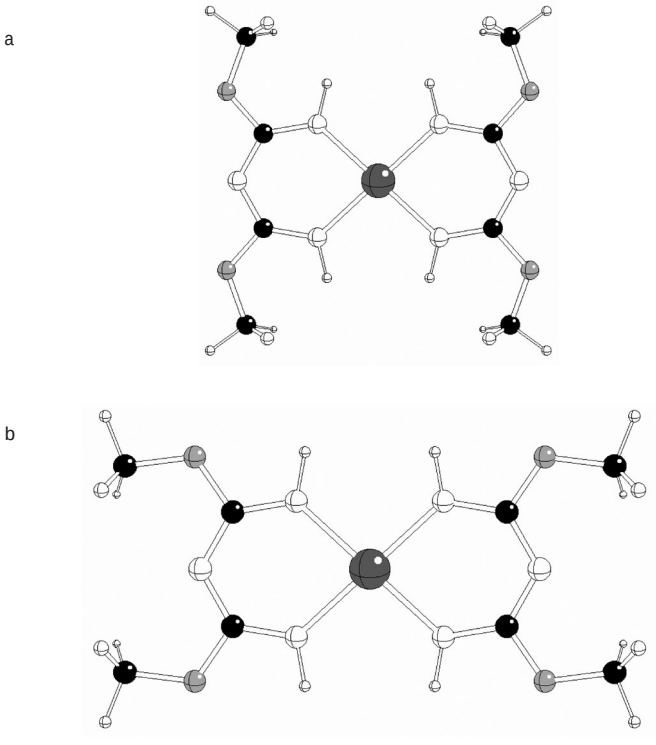

FIG. 3
Structure of $[Cu(mici)_2]$: a model C1; b model C2 (lit.[4]) (for atom notation, see Chart 2)

Hmici deprotonation (or mici$^-$ protonation) proceeds in free ligand molecules or in their transition metal complexes. The aim of our study is (i) to solve this problem using quantum-chemical treatment and (ii) to investigate mutual relations between geometry and electronic structure of free ligands and their Cu(II) complexes (the nitrogen shielding by methoxy groups, π-bond significance, etc.) for both experimentally observed conformations. This might help to explain the reasons for preferential methoxy group orientations as well as the role of transition metals in the solvation.

EXPERIMENTAL

All ab initio MP2 molecular orbital calculations were performed using standard Gaussian 94 program package[13] with standard 6-31G* basis sets[14] for all atoms except Cu where 6-311G* basis set[15] was applied. Within this treatment, the geometries of all the systems under study (Table I) were optimized using Berny algorithm[16] with standard accuracy. Electronic struc-

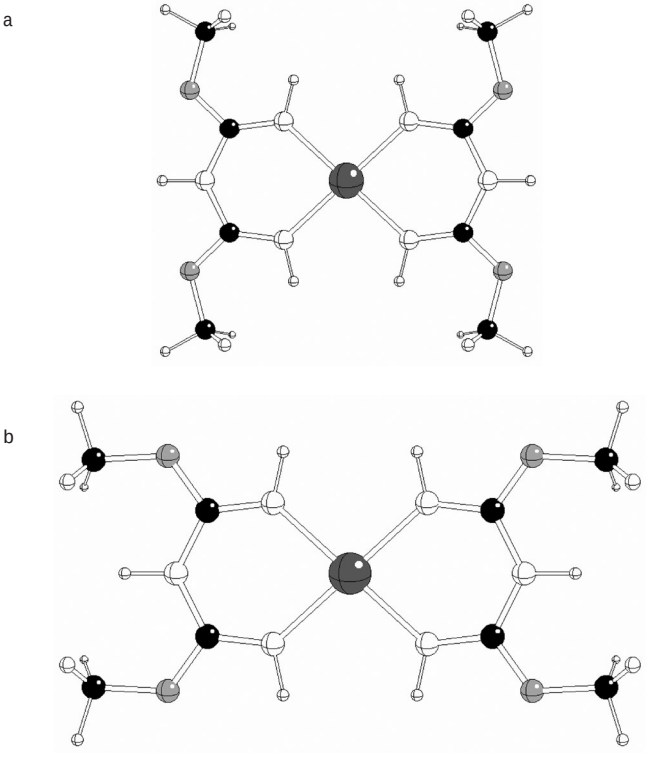

FIG. 4
Structure of $[Cu(Hmici)_2]^{2+}$: a model D1 (lit.[7]); b model D2 (for atom notation, see Chart 2)

ture was evaluated in terms of Mulliken population analysis (MPA), such as gross atomic charges for atoms and overlap populations for bonds.

Omitting the polarization *f*-type function at Cu atoms[15], topological analysis of electron density[17] has been elaborated (AIM2000 program package[18]) and the results have been evaluated in terms of electron density ρ, density Laplacian *L* and bond ellipticity ε at bond critical points (BCP), as well as in terms of atomic volumes and atomic charges evaluated using the electron density integrated over atomic basins (up to 0.001 a.u. level).

RESULTS AND DISCUSSION

The systems under study may be denoted as Xy models (Table I), where X stands for the compound (A for mici$^-$, B for Hmici, C for $[Cu(mici)_2]$ and D for $[Cu(Hmici)_2]^{2+}$) and y describes the conformation using the N(1)–C(1)–O–C(Me) dihedral angle (1 stands for 0° and 2 for 180°, see Figs 1–8 and Charts 1 and 2 for the notation of atoms).

TABLE I
Description of models and total MP2 energy data, *E*(MP2), of the systems under study (for atom notation, see Charts 1 and 2)

Model	Compound	N1–C1–O–C^{Me} dihedral angle, °	*E*(MP2), a.u.
A1	mici$^-$	0	–470.50010
A2	mici$^-$	180	–470.51796
B1	Hmici	0	–471.09226
B2	Hmici	180	–471.07119
C1	$[Cu(mici)_2]$	0	–2579.99909
C2	$[Cu(mici)_2]$	180	–2580.04141
D1	$[Cu(mici)_2]^{2+}$	0	–2580.72580
D2	$[Cu(mici)_2]^{2+}$	180	–2580.70477

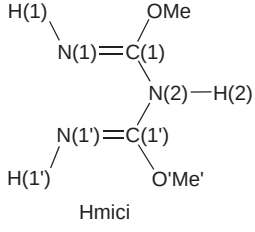

Hmici

CHART 1
Schematic description of neutral bis(methoxycarbimido)amine

Total MP2 energies of our optimized model structures in vacuo (C_{2v} symmetry for free ligands and D_{2h} symmetry for their Cu complexes as in real systems[4,7]) are collected in Table I. According to the energy data, all systems with anionic mici$^-$ ligands prefer the X1 conformation with N(2) shielded by methoxy group (Figs 1b and 3b), whereas neutral Hmici systems prefer the X2 one with N(1)–H(1) shielded (Figs 2a and 4a), in agreement with experimental structural data[4,7]. The absolute value of the energy difference between both conformations is higher for the copper complexes than the free ligands. However, the reverse relation holds, assuming that copper complexes contain two ligands (i.e., the energy difference must be halved), and so the D system is the most advantageous one for conformation changes. Similarly, the energy of deprotonation related to a single H^+ particle (the E(By) – E(Ay) and (E(Dy) – E(Cy))/2 differences, y = 1 or 2) increase in the sequence D2 < D1 < B2 < B1. Nevertheless, the energetically more advantageous deprotonation of X2 conformations with methoxy-shielded N(2)/H(2) positions in comparison with the X1 ones is in contradiction with the steric accessibility of the H(2) atom in these systems. Based on the same Cu^{2+} energy value, the relative stability of our copper complexes may be (roughly) estimated using the E(Cy) – 2E(Ay) and E(Dy) – 2E(By) differences, y = 1 or 2. Our results indicate that this stability should increase in the order C2 < D1 < D2 < C1.

The geometry of our model systems is described in Table II. The deviations of experimental X-ray data ($C2_{exp}$ (lit.[4]) and $D1_{exp}$ (lit.[7])) from the MP2-optimized structures in vacuo may be explained by influences of environment. The bond lengths deviations decreasing with the distance from the Cu center indicate additional intermolecular interactions of the Cu atoms in real structures. H atom positions in experimental structures were not corrected and the real N–H and C–H bond lengths are therefore longer

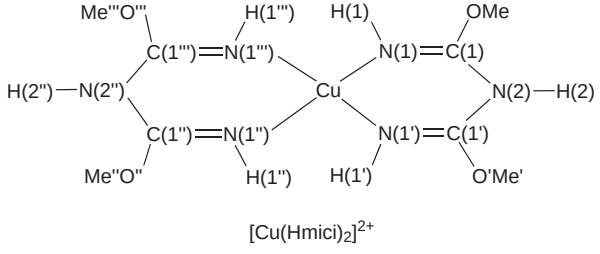

CHART 2
Schematic description of bis[bis(methoxycarbimido)amine]copper(II)

than the presented values. It may be seen that the N(1)–C(1) and C(1)–O bonds are shorter than their C(1)–N(2) and O–C(Me) counterparts, respectively. This might be related to the increased π character of the corresponding bonds. An analogous relation for the N(1)–H(1) and N(2)–H(2) bonds, possibly explaining the preferential $H(2)^+$ deprotonation, is not so evident. On the other hand, the value of the H(2)–N(1)–C(1) angle indicates an sp^3 (typical of single C–N bonds) rather than sp^2 hybridization

TABLE II
Selected bond lengths and bond angles of the system under study (see Table I)

Model	A1	A2	B1	B2	C1	C2	$C2_{exp}$ [a]	D1	$D1_{exp}$ [b]	D2
					Bond lengths, 10^{-10} m					
Cu–N1	–	–	–	–	2.036	2.037	1.945(4)	2.068	1.965(3)	2.056
N1–C1	1.300	1.297	1.274	1.271	1.324	1.318	1.299(3)	1.304	1.279(8)	1.300
C1–N2	1.344	1.348	1.385	1.394	1.332	1.338	1.329(6)	1.374	1.363(7)	1.384
C1–O	1.436	1.425	1.382	1.385	1.369	1.363	1.359(8)	1.323	1.33(7)	1.325
$O–C^{Me}$	1.406	1.417	1.427	1.425	1.425	1.436	1.434(2)	1.454	1.436(7)	1.455
N1–H1	1.022	1.028	1.020	1.024	1.016	1.020	0.74(4)	1.019	0.860(1)	1.023
N2–H2	–	–	1.011	1.004	–	–	–	1.019	0.861(1)	1.013
$C^{Me}–H^{Me}$ [c]	1.094	1.096	1.089	1.089	1.089	1.090	0.96(4)	1.086	0.96(4)	1.087
$C^{Me}–H^{Me}$	1.100	1.094	1.094	1.096	1.096	1.091	0.91(6)	1.092	0.91(6)	1.092
					Bond angles, °					
N1–Cu–N1′	–	–	–	–	85.7	85.3	88.1(1)	86.3	88.3(2)	85.1
Cu–N1–C1	–	–	–	–	127.6	127.8	126.9(2)	129.9	128.6(6)	130.8
H1–N1–C1	110.3	105.6	111.2	114.1	112.9	109.2	109(2)	111.1	115.7(3)	108.1
N1–C1–N2	131.8	132.5	124.9	124.5	128.7	129.1	128.8(4)	123.1	124.1(7)	123.0
C1–N2–C1′	121.1	121.7	129.1	127.1	121.7	120.7	120.1(1)	129.1	125.8(8)	127.3
N1–C1–O	122.8	115.7	130.0	121.4	122.0	115.0	115.4(2)	128.3	125.8(4)	119.2
N2–C1–O	105.4	111.9	105.2	114.1	109.3	115.9	115.7(2)	108.6	109.1(7)	117.8
$C1–O–C^{Me}$	116.6	116.9	115.8	121.8	118.4	117.2	117.5(4)	119.5	118.5(5)	122.9
C1–N2–H2	–	–	115.5	116.5	–	–	–	115.4	117.1(4)	116.3
$O–C^{Me}–H^{Me}$ [c]	105.8	105.2	105.2	105.1	105.0	104.5	106.4(4)	104.2	109.4(1)	104.1
$O–C^{Me}–H^{Me}$	112.8	112.1	111.2	111.9	111.6	110.9	111(3)	109.9	109.5(1)	110.3
$H^{Me}–C^{Me}–H^{Me}$	108.0	107.8	109.8	110.4	109.2	110.6	105(2)	112.2	109.5(1)	112.6
$H^{Me}–C^{Me}–H^{Me}$ [c]	108.7	109.8	109.7	108.6	109.2	110.6	117.4(4)	110.2	109.5(1)	109.6

[a] Averaged X-ray data[4] (standard deviations in parentheses). [b] Averaged X-ray data[7] (standard deviations in parentheses). [c] H^{Me} in the molecule plane.

at the N(1) atoms (cf. also O–C^{Me}–H^{Me} bond angles). In the Hmici systems, the N(1)–C(1)–N(2) bond angles are significantly smaller than the C(1)–N(2)–C(1′) ones, whereas the reverse relation holds in the $mici^-$ systems. This might be explained by the shift in the delicate balance of ring strain between the C(1) and N(2) atoms due to the splitting of $H(2)^+$ (the N(2) center in Hmici is less rigid than the C(1) one but the reverse relation holds after the splitting of $H(2)^+$ in $mici^-$).

Selected MPA electronic structure parameters are presented in Table III. The nitrogen charges are more negative than the oxygen ones (especially in Cu complexes). Also the C^{Me} atoms bear negative charges, unlike the C(1) ones. Slightly more positive H(2) charges compared to H(1) ones could explain their preferential deprotonation. The N–H bonds are more polar in the copper complexes than in the free ligands. The spin data in the Cu(II) complexes indicate that the unpaired electron is localized at the central Cu atoms, and this may be supported by their d electron populations. The N(1)–C(1) bonds are stronger than C(1)–N(2) ones in the Hmici systems, whereas the reverse relation holds in the $mici^-$ systems. The C(1)–O bonds are stronger than their O–C^{Me} counterparts. There are no significant differences between the N(1)–H(1) and N(2)–H(2) bonds that could explain the preferential $H(2)^+$ splitting.

Another piece of information may be found in AIM electronic structure parameters (Tables IV and V). The MPA relation between the nitrogen and oxygen charges does not hold for all the systems. The C(1) electron density is lower than the C^{Me} one, in agreement with the MPA treatment but, unlike in MPA, all the carbon atoms have positive charges. The MPA relation between the positive hydrogen charges is also valid.

Atomic volumes usually increase with electron density on atoms as well as with the mechanical strain[17]. N(1), C^{Me} and H(1) atomic volumes are larger than their N(2), C(1) and H(2) counterparts, respectively. The increased N(2) volumes in $mici^-$ systems may be ascribed to the missing H(2) atoms as well as to a higher mechanical strain, whereas the same for the C(1) volumes is caused exclusively by the increased mechanical strain (cf. also the trends in C(1)–N(2)–C(1′) and N(1)–C(1)–N(2) angles).

Bond strengths may be deduced also from their BCP electron density data. Unlike in MPA, the N(1)–C(1) bonds are stronger than N(2)–C(2) in all systems under study. In agreement with MPA, the strengths of all N–H bonds in the Hmici ligands are nearly equal. Except for the A systems, C(1)–O bonds are stronger than O–C^{Me}.

BCP Lagrangians are related to the bond type, their positive values indicating coordination bonding with heavy atoms (like in Cu–N(1) bonds),

TABLE III
Selected MPA parameters of the systems under study (see Table I)

Model	A1	A2	B1	B2	C1	C2	D1	D2
				Atomic charges				
Cu	–	–	–	–	1.059	1.043	1.169	1.161
N1	–0.664	–0.664	–0.583	–0.571	–0.849	–0.825	–0.833	–0.812
N2	–0.618	–0.697	–0.758	–0.810	–0.514	–0.612	–0.762	–0.822
C1	0.561	0.612	0.680	0.699	0.713	0.749	0.882	0.894
C^{Me}	–0.214	–0.169	–0.254	–0.265	–0.257	–0.289	–0.294	–0.306
O	–0.510	–0.563	–0.522	–0.518	–0.488	–0.540	–0.480	–0.486
H1	0.253	0.249	0.317	0.319	0.338	0.343	0.385	0.397
H2	–	–	0.394	0.395	–	–	0.457	0.445
H^{Me} [a]	0.135	0.108	0.196	0.210	0.204	0.176	0.274	0.279
H^{Me}	0.123	0.138	0.174	0.167	0.166	0.176	0.214	0.216
				Spin				
Cu	–	–	–	–	0.995	0.995	1.003	1.002
				d electron population				
Cu	–	–	–	–	8.884	8.884	8.889	8.887
				Overlap populations				
Cu–N1	–	–	–	–	0.189	0.188	0.162	0.163
N1–C1	0.504	0.538	0.574	0.602	0.318	0.366	0.394	0.427
C1–N2	0.410	0.353	0.218	0.176	0.473	0.424	0.288	0.251
C1–O	0.230	0.223	0.281	0.252	0.309	0.299	0.379	0.360
$O–C^{Me}$	0.215	0.213	0.202	0.192	0.208	0.206	0.172	0.167
N1–H1	0.254	0.250	0.288	0.275	0.280	0.283	0.300	0.295
N2–H2	–	–	0.288	0.290	–	–	0.294	0.292
$C^{Me}–H^{Me}$ [a]	0.371	0.351	0.378	0.381	0.380	0.368	0.377	0.377
$C^{Me}–H^{Me}$	0.351	0.365	0.364	0.357	0.357	0.369	0.363	0.361

[a] H^{Me} in the molecule plane.

whereas the high negative values are characteristic of covalent bonds in our systems (bonds of the "shared" type)[17]. In the Hmici systems, the L_{BCP} values of the N(1)–C(1) bonds are more negative than those of their C(1)–N(2) counterparts, whereas in the mici$^-$ systems the reverse relation holds. Except for the A systems, L_{BCP} values of the C(1)–O bonds are more negative than those of the O–C^{Me} bonds. The N(2)–H(2) bonds have the most negative L_{BCP} values among all the systems under study.

TABLE IV
Selected atomic AIM parameters of the systems under study (see Table I)

System	A1	A2	B1	B2	C1	C2	D1	D2
				Charges				
Cu	–	–	–	–	1.35	1.34	1.40	1.40
N1	–1.04	–1.01	–1.01	–1.13	–1.16	–1.14	–1.32	–1.30
N2	–0.99	–1.09	–1.06	–1.09	–0.97	–1.05	–1.32	–1.32
C1	1.73	1.72	1.85	1.81	1.90	1.90	1.98	1.96
C^{Me}	0.55	0.54	0.42	0.43	0.43	0.50	0.34	0.34
O	–0.99	–1.03	–1.03	–1.04	–1.02	–1.06	–1.11	–1.11
H1	0.41	0.33	0.38	0.40	0.38	0.40	0.43	0.46
H2	–	–	0.48	0.43	–	–	0.53	0.48
H^{Me} [a]	0.04	0.03	0.10	0.11	0.10	0.08	0.16	0.17
H^{Me}	0.04	0.06	0.07	0.07	0.09	0.09	0.10	0.10
				Spin density, a.u.				
Cu	–	–	–	–	–0.077	–0.077	–0.080	–0.076
				Volumes, a.u.				
Cu	–	–	–	–	85.8	86.2	83.4	93.2
N1	130.1	130.7	127.9	128.3	114.4	115.0	116.6	115.7
N2	110.8	102.5	91.9	92.5	106.6	103.8	95.0	95.6
C1	37.5	36.5	34.5	35.2	33.4	33.0	30.6	31.0
C^{Me}	59.5	60.3	63.7	62.8	63.0	62.3	67.1	66.6
O	97.3	98.6	96.9	98.0	96.8	97.8	96.6	97.6
H1	31.6	34.9	29.6	30.8	28.0	29.8	26.8	26.9
H2	–	–	24.5	21.2	–	–	22.3	21.4
H^{Me} [a]	49.4	50.8	45.7	44.8	45.5	46.8	40.8	40.5
H^{Me}	49.5	48.0	47.2	47.8	47.3	46.2	44.4	44.4

[a] H^{Me} in the molecule plane.

TABLE V
Selected BCP AIM parameters of the systems under study (see Table I)

System	A1	A2	B1	B2	C1	C2	D1	D2
				ρ_{BCP}, a.u.				
Cu–N1	–	–	–	–	0.082	0.081	0.076	0.078
N1–C1	0.372	0.379	0.393	0.399	0.354	0.362	0.371	0.377
C1–N2	0.346	0.340	0.309	0.300	0.354	0.348	0.318	0.309
C1–O	0.245	0.252	0.281	0.276	0.288	0.292	0.322	0.319
O–C^{Me}	0.268	0.258	0.245	0.247	0.249	0.239	0.219	0.219
N1–H1	0.319	0.315	0.320	0.316	0.323	0.319	0.319	0.315
N2–H2	–	–	0.325	0.334	–	–	0.315	0.324
C^{Me}–H^{Me} [a]	0.275	0.273	0.281	0.280	0.280	0.280	0.284	0.284
C^{Me}–H^{Me}	0.271	0.276	0.276	0.275	0.275	0.279	0.279	0.278
				L_{BCP}, a.u.				
Cu–N1	–	–	–	–	0.287	0.287	0.263	0.272
N1–C1	–1.190	–1.258	–1.179	–1.243	–1.124	–1.186	–1.176	–1.234
C1–N2	–1.259	–1.227	–1.040	–0.971	–1.309	–1.265	–1.073	–1.008
C1–O	–0.499	–0.490	–0.526	–0.501	–0.484	–0.465	–0.442	–0.434
O–C^{Me}	–0.596	–0.512	–0.344	–0.404	–0.430	–0.346	–0.156	–0.183
N1–H1	–1.457	–1.443	–1.530	–1.520	–1.549	–1.538	–1.559	–1.547
N2–H2	–	–	–1.623	–1.660	–	–	–1.579	–1.618
C^{Me}–H^{Me} [a]	–0.955	–0.935	–1.019	–1.023	–1.072	–1.002	–1.082	–1.082
C^{Me}–H^{Me}	–0.917	–0.965	–0.973	–0.956	–0.954	–0.998	–1.007	–1.001
				ε_{BCP}				
Cu–N1	–	–	–	–	0.065	0.066	0.077	0.083
N1–C1	0.338	0.368	0.401	0.443	0.245	0.270	0.297	0.336
C1–N2	0.194	0.179	0.198	0.194	0.182	0.162	0.168	0.152
C1–O	0.028	0.025	0.069	0.081	0.045	0.042	0.092	0.100
O–C^{Me}	0.015	0.025	0.002	0.013	0.005	0.007	0.035	0.042
N1–H1	0.002	0.002	0.006	0.006	0.014	0.015	0.011	0.010
N2–H2	–	–	0.043	0.006	–	–	0.035	0.036
C^{Me}–H^{Me} [a]	0.034	0.038	0.038	0.037	0.036	0.039	0.039	0.039
C^{Me}–H^{Me}	0.034	0.032	0.041	0.044	0.041	0.037	0.048	0.050

[a] H^{Me} in the molecule plane.

BCP ellipticities increase with the π character of the bond (up to the double bonds) but they may also reflect the increasing mechanical strain[17]. N(1)–C(1) bond ellipticities are significantly higher than those of C(1)–N(2), which may be explained by increased π bonding. Nevertheless, a comparison with the corresponding BCP electron densities implies that the mechanical strain influence cannot be excluded. C(1)–O bond ellipticities are higher than those of their O–C^{Me} counterparts, which may be explained by σ bonding with small π contributions in C(1)–O bonds from neighboring C–N bonds. Higher ellipticities of the σ-type N(2)–H(2) bonds in comparison with the N(1)–H(1) bonds may also be explained in this way.

The Cu(II) complex formation (vs free ligands) is associated with an increase in N(1)–C(1), O–C^{Me} and N(2)–H(2) bond lengths as well as in N(2)–C(1)–O and C(1)–O–C^{Me} bond angles, whereas the C(1)–N(2), C(1)–O and C^{Me}–H^{Me} bond lengths and the N(1)–C(1)–N(2), N(1)–C(1)–O and O–C^{Me}–H^{Me} bond angles exhibit the reverse trend. According to MPA, this should be associated with weaker N(1)–C(1) and O–C^{Me} bonds and stronger other bonds (except C^{Me}–H^{Me}) as well as with higher atomic charges (except N(2) and O ones). In the terms of the AIM treatment, the situation is not so simple and these trends do not hold for the N–H bonds and the C^{Me} and H(1) atomic charges. Lower N–C bond strength alternation in the copper complexes within the AIM treatment is associated with more negative L_{BCP} and lower ε_{BCP} data (higher shared and lower π characters) whereas higher values of both these quantities are typical of the C–O and N(2)–H(2) bonds. Nevertheless, the H(2) atomic charges increase with the Cu complex formation in both treatments. The decreased N(1) atomic volume – despite higher negative atomic charges – may be explained by steric reasons (additional copper atom), whereas the C atomic volume changes may be explained by reverse changes in their positive atomic charges.

The H(2) deprotonation is associated with shorter Cu–N(1), C(1)–N(2) and O–C^{Me} bonds and lower Cu–N(1)–C(1), C(1)–N(2)–C(1′) and N(1)–C(1)–O bond angles, whereas the other bond lengths as well as the N(1)–C(1)–N(2) and O–C^{Me}–H^{Me} bond angles increase. MPA associates this process with decreasing polarization of all atoms except N(1) and O. AIM confirms these trends for the N(2), C(1) and H^{Me} charges only, whereas the reverse relations should hold for the C^{Me} atoms. The deprotonation should be associated with increased atomic volumes of almost all atoms, which indicates higher mechanical strain at the N(2) atoms. The mentioned bond length trends are (with some exceptions) well reflected by bond strength trends in MPA and AIM treatments (longer bonds are weaker and vice

versa). A significant ε_{BCP} decrease in the N(1)–C(1) bond is associated with bond weakening, but with bond strengthening in the C(1)–O bond, which indicates different π character of these bonds.

The effect of the methoxy group positions is manifested by large changes in N(1,2)–C(1)–O bond angles but the other centers are also influenced. N(2) positions shielded by the methoxy groups shorten the N(1)–C(1) and lengthens C(1)–N(2) bonds. This is associated with increasing MPA polarity of these bonds, whereas this trend is not observed within the AIM treatment. Longer (shorter) C–N bonds are reflected by lower (higher) MPA and AIM bond strengths and bond ellipticities. Shielding N(2) positions by methoxy groups is associated with a shorter and stronger N(2)–H(2) bond as well as with higher MPA charge of H(2) but its AIM charge and atomic volume decreases (this may be explained by steric effects of both methoxy groups). This is accompanied also by increasing Cu, O and H(1) atomic volumes. Consequently, the X2 isomers are less suitable for H(2) deprotonation than their X1 counterparts, not only due to steric reasons.

Finally, it may be concluded that MPA and AIM treatments exhibit different trends in many cases. According to the authors' opinion, the MPA results are less reliable, which might be partly ascribed to the non-physical origin of the polarization functions used. In agreement with experimental data, the preferred conformation of our systems depends on the ligand ($mici^-$ prefers the X2 conformation whereas Hmici prefers the X1 one). The mechanical strain equilibrium between the C(1) and N(2) atoms is changed due to increased π bonding for the C(1)–N(2) bond in $mici^-$ as a consequence of the $H(2)^+$ splitting, and the more rigid N(2) atom explains the observed geometry differences. Deprotonation depends more on the H charges than on the N–H bond strengths. The shielding by the methoxy group is the main reason for the preferred site of deprotonation (based on both steric and electronic structural arguments). Energy as well as electronic structure arguments indicate that the deprotonation of the $[Cu(Hmici)_2]^{2+}$ complex is more probable than that of the free Hmici ligand. As the X1 conformations of the complex are the most stable ones, the deprotonation occurs in the H(2) position.

As mentioned above, the relative stability of the transition metal complexes with the neutral Hmici and anionic $mici^-$ ligands depends also on the influence of the solvent. Unfortunately, recent Gaussian program packages can include solvent effects using various versions of polarized continuum models based on dipoles (and higher multipoles), which are not suitable for charged systems[19]. Consequently, more sophisticated models of solvent effect inclusion are necessary for this type of studies. Finally, it may be

concluded that our work is the initial step in solving a very complex problem and further theoretical as well as experimental studies in this field are desirable.

This work was supported by Science and Technology Assistance Agency under the contract No. APVT-20-005702. Slovak Grant Agency VEGA (contract No. 1/0052/03) is acknowledged for partial financial support. We thank IBM Slovakia Ltd. for computing facilities.

REFERENCES

1. Kohout J., Jäger L., Hvastijová M., Kožíšek J.: *J. Coord. Chem.* **2000**, *51*, 169.
2. *Gmelins Handbuch der Anorganischen Chemie. 8. Auflage. 14. Kohlenstoff. Teil D1. Kohlenstoff-Stickstoff-Verbindungen* (D. Koschel, Ed.), p. 295. Verlag Chemie, Weinheim 1971.
3. Kožíšek J., Hvastijová M., Kohout J.: *Inorg. Chim. Acta* **1990**, *168*, L157.
4. Boča R., Hvastijová M., Kožíšek J., Valko M.: *Inorg. Chem.* **1996**, *35*, 4794.
5. Boča R., Hvastijová M., Kožíšek J.: *J. Chem. Soc., Dalton Trans.* **1995**, 1921.
6. Fronc M., Kožíšek J., Breza M., Hvastijová M., Svoboda I., Duarte M. T.: *Crystallography in Natural Sciences and Technology* (K. Stadnicka and W. Nitek, Eds), p. 167. EJB Publisher, Krakow 2001.
7. Bishop M. M., Lindoy L. F., Mahadev S., Turner P.: *J. Chem. Soc., Dalton Trans.* **2000**, 233.
8. Brudíková K., Breza M.: *Polyhedron* **2004**, *23*, 2235.
9. Freeman H. C., Smith J. E. W. L., Taylor J. C.: *Acta Crystallogr.* **1961**, *14*, 407.
10. Birker P. J. M. W. L., Smits J. M. M., Bour J. J., Beurskens P. T.: *Rec. Trav. Chim. Pays-Bas* **1973**, *92*, 1240.
11. Pajunen A., Pajunen S.: *Acta Crystallogr., Sect. C: Cryst. Struct. Commun.* **1994**, *50*, 1884.
12. Allen F. H.: *Acta Crystallogr., Sect. B: Struct. Sci.* **2002**, *58*, 380.
13. Frisch M. J., Trucks G. W., Schlegel H. B., Gill P. M. W., Johnson B. G., Robb M. A., Cheeseman J. R., Keith T. A., Petersson G. A., Montgomery J. A., Raghavachari K., Al-Laham M. A., Zakrzewski V. G., Ortiz J. V., Foresman J. B., Cioslowski J., Stefanov B. B., Nanayakkara A., Challacombe M., Peng C. Y., Ayala P. Y., Chen W., Wong M. W., Andres J. L., Replogle E. S., Gomperts R., Martin R. L., Fox D. J., Binkley J. S., Defrees D. J., Baker J., Stewart J. P., Head-Gordon M., Gonzales C., Pople J. A.: *Gaussian 94*, Revision D.1. Gaussian Inc., Pittsburgh (PA) 1995.
14. Hariharan P. C., Pople J. A.: *Theor. Chim. Acta* **1973**, *28*, 213.
15. a) Wachters A. J. H.: *J. Chem. Phys.* **1970**, *52*, 1033; b) Bauschlicher C. W., Jr., Langhoff S. R., Barnes L. A.: *J. Chem. Phys.* **1989**, *91*, 2399.
16. Peng C., Ayala P. Y., Schlegel H. B., Frisch M. J.: *J. Comput. Chem.* **1996**, *17*, 49.
17. Bader R. F. W.: *Atoms in Molecules: A Quantum Theory*. Clarendon Press, Oxford 1990.
18. a) Biegler-König F., Schönbohm J., Bayles D.: *J. Comput. Chem.* **2001**, *22*, 545; b) http://www.aim2000.de/
19. Buckingham A. D.: *Adv. Chem. Phys.* **1967**, *12*, 107.